# Experimental Study on Effects of Tornado on Roofing System in Low-rise Building

Hitomitsu KIKITSU[1] and Partha P. SARKAR[2]

ABSTRACT

This paper presents the results of experimental studies on transient wind loads on a low-rise building induced by a tornado. The Tornado Simulator at Iowa State University was used for the experiments. The internal pressure was considered for improved prediction of the dynamic wind loads. It is shown that the magnitude of internal pressure determines the total wind uplift force on the roof and that its characteristics depend on the extent of background leakage in the building walls as well as location of dominant openings on any of these walls. Further, the authors tried to develop the model for wind force coefficients on the roofing based on the Rankine vortex model. It was shown that the model can agree with the characteristics of the experimental results by applying appropriate values on the related parameters.

KEYWORDS: Tornado Simulator, Rankine Vortex Model, Wind Force Coefficient, Roofing System

## 1.0 INTRODUCTION

Tornadoes produce rotating winds with updraft and downdraft and radial flows that intensify significantly near the ground. In most commonly occurring tornadoes that are EF-2 or of less intensity on the newly implemented Enhanced Fujita Scale, winds could reach 60 m/s (or 135 mph) near the ground. The importance of internal pressure inside a building in modifying the resultant uplift force on the roofing system was generally recognized, but has not been explored because of some limitations in the model geometry. It is known that the internal pressure inside a building is a function of air leakage through the building envelope because of intrinsic porosity present in the envelope and any dominant opening that could be triggered by a puncture in the envelope by wind-borne debris.

This paper studies the role of internal pressure in producing the resultant wind loads in a tornado-like vortex as a

1 Senior Researcher, National Institute for Land and Infrastructure Management, MLIT, 1 Asahi, Tsukuba, Ibaraki 305-0044 JAPAN

2 Professor, College of Engineering, Iowa State University, 2271 Howe Hall, Ames, IA 50011 USA

function of porosity and dominant opening in a building envelope. First experimental results using ISU Tornado Simulator shown in Figure.1 is summarized. The detailed specification of the simulator is given in Haan, et al.(2008). Furthermore, the authors tried to develop the model for wind force coefficients on the roofing based on the Rankine vortex model by reflecting the experimental results on it.

## 2.0 PAST EXPERIMENTS USING ISU TORNADO SIMULATOR

### 2.1 Pressure Model Details

This section summarizes past experiments by Kikitsu, H et al.(2009). Tornado-induced surface pressures were measured on a low-rise building model with 152.4mm by 97.5mm in plan dimensions and an eave height of 48.8mm. The shallow roof angle of the model was 1/12 ($4.76^0$) with the roof ridge parallel to the longer dimension. The configuration of this model is the same as that used in the study by Oh et al. (2007). The model was made out of plexiglass and contained 20 pressure taps on roof surface and 16 ones on four walls to measure the external pressure distribution and a single pressure tap to measure the internal pressure.

The geometric and velocity scale ratios were 1/250 ( $\lambda_L$ ) and 1/10 ( $\lambda_{Vel}$ ), respectively. The internal volume of the model was scaled also to maintain similarity of the dynamic response of the volume at model scale to that in full scale. The internal volume scale ($\lambda_{Vol}$), as defined below, was calculated as follows:

$$\lambda_{Vol} = \frac{{\lambda_L}^3}{{\lambda_{Vel}}^2} = \frac{1}{156{,}250} \quad . \tag{1}$$

In order to achieve this scale, a sealed volume chamber was installed at the bottom of the model so that its internal volume was increased proportionately based on the scaling law above.

Dominant openings and leakage on the walls were taken into consideration to evaluate the characteristics of internal pressure during the passage of a tornado with the building placed along the centerline of the tornado path. The building was oriented with its shorter wall normal to the translation direction of the tornado as shown in Figure 2. Table 1 shows the geometry and ratio of dominant openings and leakage, where the opening ratio (*r*) is defined as area of the opening to the total surface area of the building walls. Distributed leakage in a real building will be distributed uniformly on the building envelope, comprising of walls and roof, and is representative of the porosity that naturally occurs in the building material.

### 2.2 Characteristics of Wind Force on the Roofing System

Figures 3 and 4 show the results of wind force coefficients in $z$ direction as obtained from the pressure coefficients. Horizontal axis in these figures is the distance between the center of the tornado vortex and the center of the building model, $x$, normalized by the radius of the tornado core, $R_m$.

2.2.1 Experimental Cases Where There is Only Distributed leakage on Each Wall (See Figure 3)

Absolute value of external wind pressure coefficient, $C_{pe}$, increased as the simulator approached the model. It became maximum when $x/R_m$ was approximately ±1.0 and minimum when $x/R_m$ was zero. In contrast, absolute value of internal wind pressure coefficient, $C_{pi}$, became maximum when $x/R_m$ was zero where the maximum value increased with the opening ratio ($r$) of distributed leakage which resulted in the maximum value of wind force coefficient, $C_{Fz}$, at $x/R_m$ of ≈±1.0; these values were around 2.6 in the case of $r$=0.04% and around 1.8 in the case of $r$=0.13%, respectively.

2.2.2 Experimental Cases Where There is Distributed Leakage ($r$=0.13%) on Each Wall and a Dominant Opening on One Wall (See Figure 4)

In the experimental cases where there was not only distributed leakage but also a dominant opening on one wall, it was found that characteristics of the wind force on the roof depend on the location of the dominant opening. First, for the cases of dominant opening on wall #1 or #4, the value of $C_{Fz}$ became maximum when $x/R_m$ was ≈1.0, since the absolute value of $C_{pi}$ was bigger when $x/R_m$ was negative. In contrast, for the cases of dominant opening on wall #2 or #3 the characteristics of $C_{Fz}$ showed different tendency from those above and it became maximum when $x/R_m$ was ≈ −1.0.

The value of $C_{Fz}$ in each case discussed above was zero, when the center of vortex reached the center of model. The value of $C_{pi}$ in each case had high correlation with the value of $C_{pe}$ of the tap that was nearest to the dominant opening.

3.0 MODELING OF TORNADO-INDUCED FORCE ON A ROOFING SYSTEM

Generally, tornado-induced aerodynamic force on a structure may be divided into two effects as shown in Figure 5: effect induced by atmospheric pressure change and effect by wind pressures. The latter one is caused by the direct action upon the structure of the air flow, while the former one is associated with the variation of the atmospheric pressure field as the tornado moves over the structure. The past proposed models, which are based on Rankine vortex model, can characterize fundamental tornado-related wind forces, but they don't explicitly

associate the effects of internal force with the extent of background leakage or location of dominant opening.

The authors tried to develop fundamental model for tornado-induced aerodynamic force on a roofing system by reflecting the ISU experimental results on the related parameters in the model.

3.1 Past Study on the Modeling of Tornado-Induced Wind Force

Simiu, E et al.(1996) proposed the expression of total pressure due to the direct action of wind and to the atmospheric pressure change as shown below:

$$F(x)=\begin{cases}\frac{1}{2}\rho V_m^2\left[2+\frac{x^2}{R_m^2}\left(K^2C-1\right)\right] & \left(|x|\le R_m\right)\\ \frac{1}{2}\rho V_m^2\,\frac{R_m^2}{x^2}\left(1+K^2C\right) & \left(|x|>R_m\right)\end{cases} \tag{2}$$

Where $\rho$ : air pressure density, $V_m$ : maximum tangential wind velocity, $R_m$ : radius of maximum rotational wind velocity, $K$ : a constant of proportionality, $C$ : pressure coefficient, respectively. In this expression, the meaning of constant $K$ is not explicitly defined. The reduction (or size) coefficient that accounts for the non-uniformity in space of the tornado wind field is taken into consideration in the coefficient $C$. Parameters related to internal pressure such as opening ratio is not explicitly included in this expression.

3.2 Development of the Model

Wind force affecting on the roof, $F_Z$, can be expressed by the summation of atmospheric pressure change effect and wind pressure as indicated above. When the reference wind pressure is defined by the maximum tangential wind velocity, $V_m$, wind force coefficient, $C_{Fz}$, can be expressed by the related wind force coefficients.

$$F_Z(x)=F_a(x)+F_w(x)=\frac{1}{2}\rho V_m^2\;C_{Fz}(x) \tag{3}$$

$$C_{Fz}(x)=C_a(x)+C_w(x) \tag{4}$$

where $\rho$ : air pressure density, $C_a$ : wind force coefficient related to atmospheric pressure change effect, $C_w$ : wind force coefficient related to wind pressure, respectively.

In the following, wind force coefficient, $C_{Fz}$, is modeled on the basis of Rankine vortex model, reflecting the experimental results on it.

3.2.1 Wind Force Induced by Atmospheric Pressure Change, $F_a$

External wind pressure coefficient induced by atmospheric pressure change has been already formulated in the past model. Then as shown in Figure 6(*a*), the characteristics of internal wind pressure coefficient in the case where there are only distributed leakage has the same tendency as the formulated coefficient. Therefore, the past model can be modified as shown in Eq.(5) by considering the effect of internal wind pressure through distributed leakage on walls.

$$C_a(x) = C_{ae}(x) - C_{ai}(x) = \begin{cases} -(1-\varepsilon_r)\left[2 - \dfrac{x^2}{R_m^2}\right] & (|x| \le R_m) \\ -(1-\varepsilon_r)\dfrac{R_m^2}{x^2} & (|x| > R_m) \end{cases} \tag{5}$$

Where $\varepsilon_r$ is the ratio of maximum of $|C_{ai}|$ to maximum of $|C_{ae}|$. As shown in Figure 6(*a*), the ratio $\varepsilon_r$ can be estimated as 0.2 for the leakage ratio $r$ of approx. 0.04%, 0.9 for $r$ of approx. 0.13%, respectively. Therefore, this equation can explicitly indicate that the absolute value of wind force induced by atmospheric pressure change decreases with the increase of distributed leakage.

3.2.2 Wind Force Caused by Direct Action of the Air Flow, $F_w$

(1) When There Is Distributed Leakage on Each Wall

Wind force coefficient related to wind pressure, which is caused by the direct action of the flow upon the roof, can be expressed as in Eq.(6.1). Since internal pressure effect has been already considered in Eq.(5), external wind pressure effect is only included in Eq.(6.1).

$$C_w(x) = C_{we}(x) = \begin{cases} \dfrac{x^2}{R_m^2} C_{we}^* & (|x| \le R_m) \\ \dfrac{R_m^2}{x^2} C_{we}^* & (|x| > R_m) \end{cases} \tag{6.1}$$

Figure 6(*b*) shows wind force coefficient by Eq.(6.1) and corresponding external wind pressure coefficient, obtained by subtracting $C_{ae}(x)$ from experimental external wind pressure coefficient. If negative 1.6 is substituted for $C_{we}^*$ agreeing with the minimum value of experimental result, the tendency of wind pressure coefficient by Eq.(6.1) can be well consistent with that of the experimental result.

(2) When There Is a Dominant Opening on a Wall as Well as Leakage

When there is a dominant opening on a wall, it is necessary to consider the effect of internal pressure through the opening on the wind force coefficient as shown in Eq.(6.2).

$$C_w(x) = C_{we}(x) - C_{wi}(x) = \begin{cases} \dfrac{x^2}{R_m^2} C_{we}^* - C_{wi}(x) & \left(|x| \le R_m\right) \\ \dfrac{R_m^2}{x^2} C_{we}^* - C_{wi}(x) & \left(|x| > R_m\right) \end{cases} \tag{6.2}$$

Where external wind pressure coefficient at the pressure tap nearest to the opening is applied to the coefficient $C_{wi}$, since experimental result shows that they are well correlated each other.

3.2.3 Wind Force Considering Internal Wind Pressure Through Leakage And a Dominant Opening, $F_Z$

When there is a dominant opening on a wall, internal pressure coefficient in AS/ANZ 1170.2 is regulated based on the ratio of dominant opening to total background leakage. This study follows the way to estimate internal pressure through a dominant opening and background leakages. As shown in Eq.(7), internal pressure coefficient $C_i$ is formulated using $\alpha_i$ (from 0 to 1.0), degree of the contribution of air flow through background leakage to internal pressure.

$$C_i(\alpha_i, x) = \alpha_i \; C_{ai}(x) + (1 - \alpha_i) C_{wi}(x) \tag{7}$$

Where $1 - \alpha_i$ is degree of the contribution of air flow through a dominant opening.
Figure 6(*c*) shows the internal pressure coefficient estimated by Eq.(7) in the case of model with a dominant opening on wall #4. The value 0.35 is applied to $\alpha_i$ in this case. This result indicates that Eq.(7) can estimate internal pressure coefficient consistent with experimental value, if appropriate value is applied to $\alpha_i$.
Based on Eqs.(5), (6.2), and (7), wind force coefficient $C_{Fz}$ for the roof of the model with a dominant opening as well as background leakage can be expressed as follows:

$$\begin{aligned} C_{Fz}(x) &= C_a(x) + C_w(x) \\ &= C_{ae}(x) + C_{we}(x) - C_i(\alpha_i, x) \\ &= \begin{cases} \dfrac{x^2}{R_m^2}\left(C_{we}^* - \alpha_i \varepsilon_r + 1\right) - 2(1 - \alpha_i \varepsilon_r) - (1 - \alpha_i) C_{wi}(x) & \left(|x| \le R_m\right) \\ \dfrac{R_m^2}{x^2}\left(C_{we}^* + \alpha_i \varepsilon_r - 1\right) - (1 - \alpha_i) C_{wi}(x) & \left(|x| > R_m\right) \end{cases} \end{aligned} \tag{8}$$

3.3 Comparison between Experimental Result and Model on Wind Force

Figure 7 summarizes result of comparison between experimental result and model on wind force coefficient. The value $\alpha_i$ is 1.0 for the case where there is only background leakage and 0.35 for the case where there is a dominant opening plus leakage, respectively. This comparison shows that Eq.(8) for all the opening conditions agrees with

experimental results. However, absolute value of the modeled wind force coefficient is relatively smaller than that experimentally obtained at $x/R_m$ of around 1.0, where the most rapid change of wind force is observed. This fundamental study has been based on limited experimental conditions. So in the further study, more wind pressure experiments are needed to evaluate the effect of related parameters such as translation speed, ratio of vortex core to model dimension, slope of roof, and swirl ratio to the wind force coefficient.

## 4.0 CONCLUSIONS

This paper summarizes the results of experimental studies related to wind hazard on low-rise buildings induced by tornado. The ISU Tornado Simulator at Iowa State University was used for these experiments. With respect to the results of wind pressure experiments, it was observed that the magnitude of internal pressure determines the total wind uplift force affecting the roof and that its characteristics depend on the size of leakage and location of dominant opening on the wall.

Further, the authors developed fundamental model illustrating wind force coefficient on a roofing system based on the results of experimental studies. It was shown that the model can agree with the characteristics of the experimental results by applying appropriate values on the related parameters. The authors will plan to carry out more wind pressure experiments collaboratively using ISU and NILIM Tornado Simulators as shown in Figures 1 and 8 for the development of more comprehensive wind force model. The construction of NILIM Tornado Simulator was supported by Grant-in-Aid for Scientific Research (B) (#21360273) of Japan Society for the Promotion of Science (JSPS).

## 5.0 REFERENCES

AS/ANZ1170.2. (2002). Structural design actions, Part 2: Wind actions.

Haan, F.L., Sarkar, P.P. and Gallus, W.A.(2008). "Design, Construction and Performance of a Large Tornado Simulator for Wind Engineering Applications." Engineering Structures, Vol. 30 (4), 1146-1159.

Kikitsu, H, Sarkar, P.P. and Haan, F.L. (2009). "Characteristics of Tornado-induced Wind Load on Low-rise Building Using Tornado Simulator", Wind Engineers, JAWE, Vol.34, No.2, pp.237-238. (in Japanese)

Oh, J.H., Kopp, G.A. and Inculet, D.R. (2007) "The UWO contribution to the NIST aerodynamic database for wind load on low buildings: Part 3. Internal pressures", Journal of Wind Engineering and Industrial Aerodynamics, No.95, pp.755-779.

Simiu, E et al. (1996). Wind Effects on Structures, Third edition, John Wiley & Sons, Inc., pp.551-575.

Table 1. Geometry and Ratio of Dominant Opening and Leakage

| Description of opening | | Dimension (model scale) | Opening ratio, *r* |
|---|---|---|---|
| Distributed leakage | Two holes on each wall #1, 3<br>Four holes on each wall #2, 4 | d=1mm | approx. 0.04% |
| | | d=1.8mm | approx. 0.13% |
| Dominant opening | | 20.8mm x 7.6mm (wall #1, 3)<br>32.5mm x 7.6mm (wall #2, 4) | 3.3% |


Figure 1. ISU Tornado Simulator

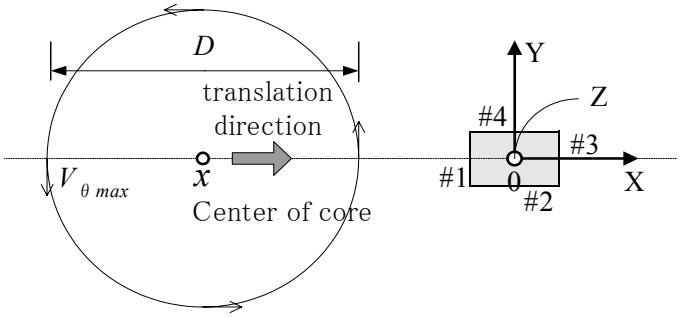


Figure 2. Definition of Wall Number and Coordinates

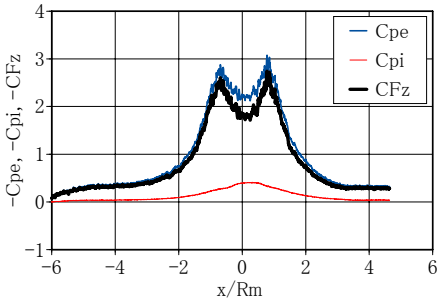


(*a*) *r* = approx.0.04%

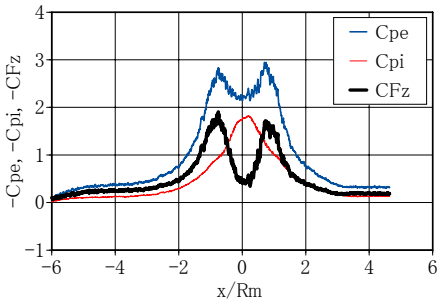


(*b*) *r* = approx.0.13%

Figure 3. Wind Force Coefficient on a Roof (When There Is Only Distributed Leakage on Walls)

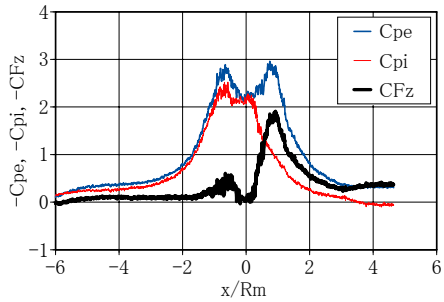


(*a*) Dominant Opening on Wall #1

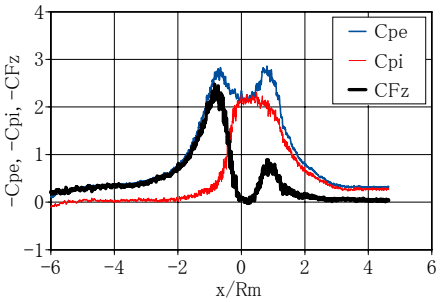


(*b*) Dominant Opening on Wall #2

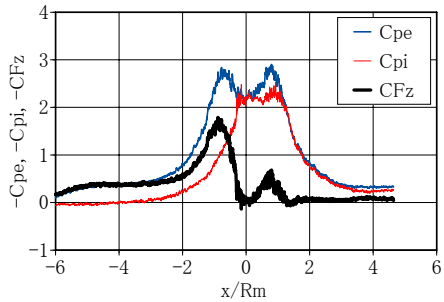


(*c*) Dominant Opening on Wall #3

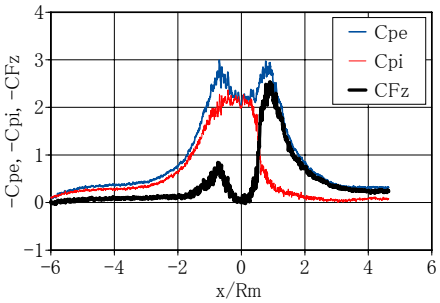


(*d*) Dominant Opening on Wall #4

Figure 4. Wind Force Coefficient on a Roof (When There is a Dominant Opening on a Wall plus Distibuted Leakage with *r* of approx. 0.13%)

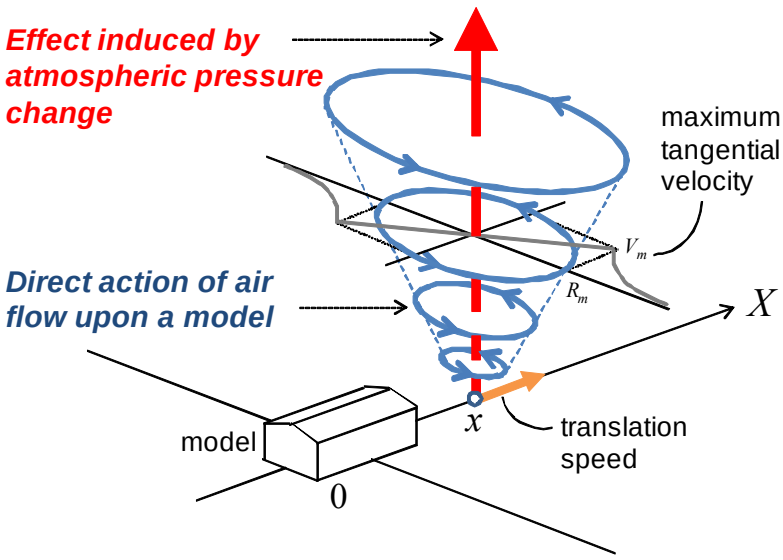


Figure 5. Diagram of Tornado-induced Aerodynamic Force Model

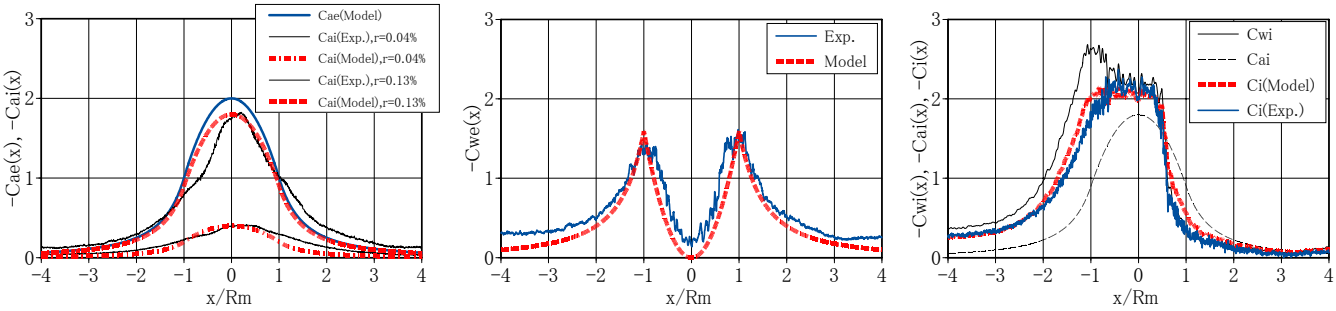


(*a*) $C_{ai}$ (*b*) $C_{we}$ (*c*) $C_i$

Figure 6. Comparison between Coefficients in Model and Experimental Results

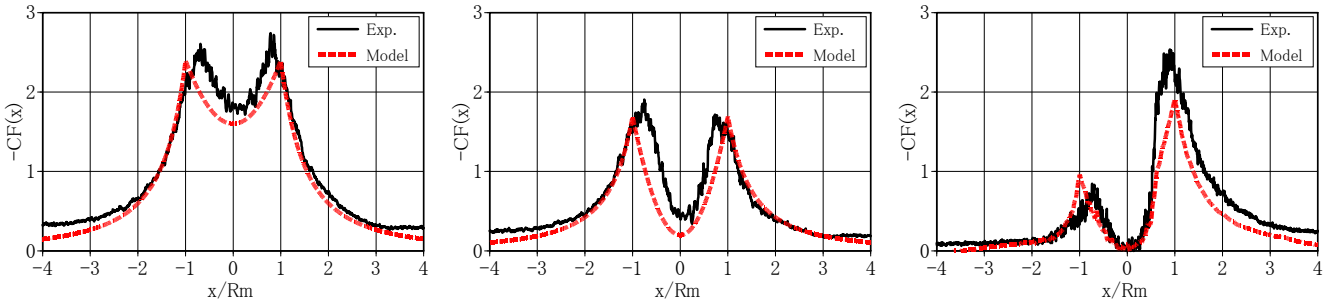


(*a*) $r$ = approx.0.04% (*b*) $r$ = approx.0.13% (*c*) $r$ = approx.0.13% + Diminant Opening on a Wall

Figure 7. Comparison between Proposed Wind Force Coefficient Model and Experimental Result

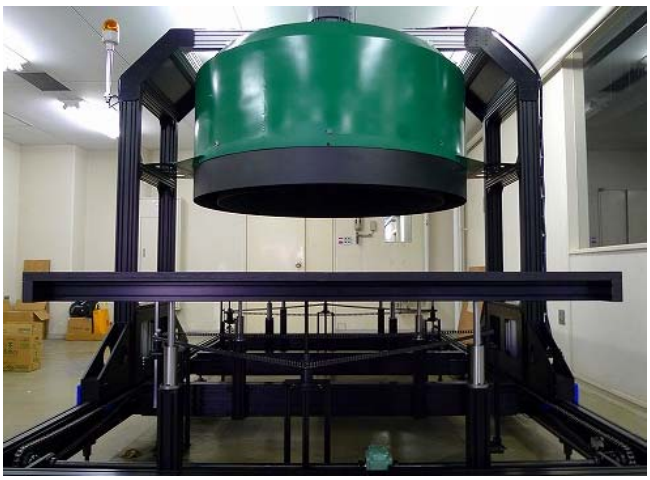

Figure 8. NILIM Tornado Simulator